Supporting information

A novel pyrazolopyridine with in vivo activity in *Plasmodium berghei* and *Plasmodium falciparum*-infected mouse models from structure-activity relationship studies around the core of recently identified antimalarial imidazopyridazines.

Claire Le Manach[†], Tanya Paquet[†], Christel Brunschwig[∞], Mathew Njoroge[∞], Ze Han[†], Diego Gonzàlez Cabrera[†], Sridevi Bashyam[ζ], Rajkumar Dhinakaran [ζ], Dale Taylor[∞], Janette Reader[¶], Mariette Botha[¶], Alisje Churchyard[¶], Sonja Lauterbach[¶], Theresa L Coetzer[§], Lyn-Marie Birkholtz[¶], Stephan Meister, Elizabeth A. Winzeler*, David Waterson[‡], Michael J. Witty[‡], Sergio Wittlin[◊,ʃ], María-Belén Jiménez-Díaz[¥], María Santos Martínez[¥], Santiago Ferrer[¥], Iñigo Angulo-Barturen[¥], Leslie J. Street[†] and Kelly Chibale[*,†,#]*

Contents:

A. Additional synthetic methods

1) 6-bromoimidazopyrimidine (5b)

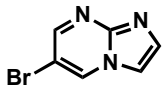

2-amino-5-bromopyrimidine (Aldrich 303526, 500 mg, 2.87 mmol, 1 eq) was dissolved in EtOH (5 mL) and water (3 mL) with bromoacetaldehyde ditehylacetal (850 µL, 4.31 mmol, 1.5 eq). HBr (500 µL) waq added. The resulting mixture was stirred at 103°C overnight. After being cooled down, it was dissolved in EtOAc and aqueous sat. $NaHCO_3$ and extracted. The organic layer was dried over Na_2SO_4 and concentrated to give 400 mg of the pure desired compound (70% yield)

^{1}H NMR (400 MHz, $CDCl_3$), δ (ppm): 8.61 (d, 1H; J = 2.4 Hz); 8.54 (d, 1H; J = 2.4 Hz); 7.84 (d, 1H; J = 1.2 Hz); 7.55 (d, 1H; J = 1.2 Hz).

2) 6-bromoimidazopyrazine (5c)

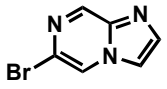

HBr (0.50 mL, 48% aqueous) was added to diethylacetal (1.5 mL, 9.89 mmol, 2 eq) and the reaction mixture was stirred at 70 ˚C for 2 h. After colling to rt, the reaction mixture was poured into *i*PrOH (20 mL) containing $NaHCO_3$ (5g, 59.5 mmol). The resulting solid was removed by filtration and 2-amino-5-bromopyrimidine (Aldrich 303526, 860 mg, 4.94 mmol, 1 eq) was added to the mother liquor. The reaction mixture was refluxed at 70 ˚C for 2 h before it was cooled to rt and quenched by the addition of $NaHCO_3$ (20 mL). *i*PrOH was removed under *in vacuo* and the aqueous mixture extracted with CH_2Cl_2 (3 x 20 mL). Combined organic extracts were dried (Na_2SO_4), filtered, and concentrated *in vacuo*. Purification by column chromatography (40-95% EtOAc/Hex) yielded 706 mg (72%) of **5c**.

^{1}H NMR (400 MHz, $CDCl_3$), δ (ppm): 8.89 (s, 1H); 8.26 (s, 1H); 7.82 (s, 1H); 7.69 (s, 1H).

3) 6-bromoimidazopyridine (5d)

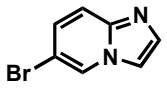

2-amino-5-bromopyridine was dissolved in EtOH/H_2O with bromoacetaldehyde diethylacetal. After addition of HBr (500 µL), the solution was heated up to 103°C overnight. The solution was cooled down and dissolved in EtOAc and water. The organic layer was washed with saturated $NaHCO_3$, dried over Na_2CO_3 and concentrated to give the desired compound (97% yield).

^{1}H NMR (400 MHz, CD_3OD), δ (ppm): 9.11 (s, 1H); 8.19 (s, 1H); 8.02 (s, 2H); 7.86 (s, 1H).

4) Synthesis of compounds (29) and (30)

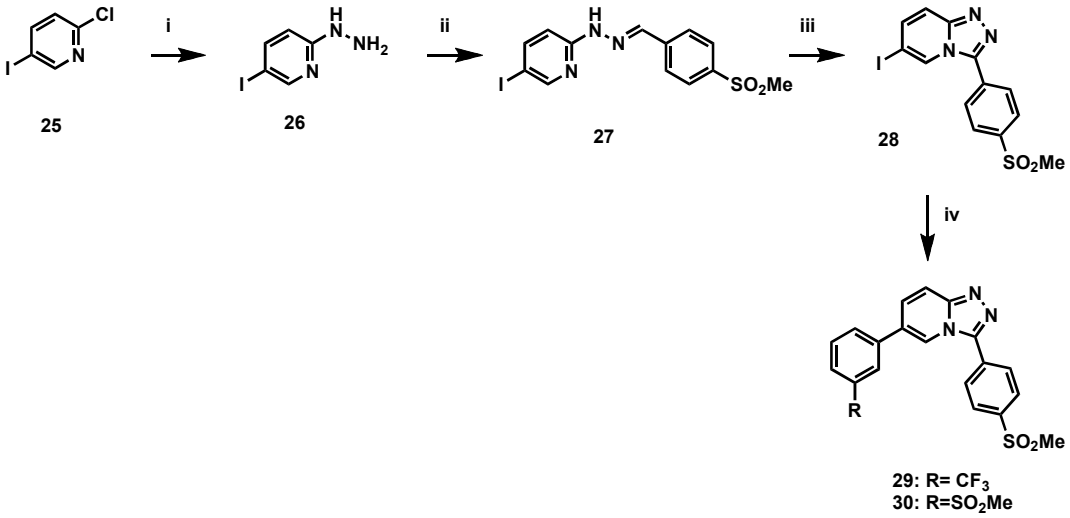

Step i: To the solution of 2-chloro-5-iodo pyridine **25** (10 g, 41.76 mmol 1 eq) in pyridine (120 mL) was added hydrazine hydrate (10.14 mL, 208.8 mmol, 5 eq) at r.t. and the mixture was heated to reflux for 16 h. Reaction mixture was cooled down to r.t. and concentrated under vacuum to yield a solid which was triturated with n-hexane (50 mL x 3) and dried to yield **26** (11.4 g, 95%) as an off white solid.

Step ii: To the suspension of **26** (11.4 g, 48.5 mmol, 1 eq) in ethanol (171 mL) was added 4-(methylsulfonyl)benzaldehyde (8.93 g, 48.5 mmol, 1 eq) at r.t. under nitrogen atmosphere and the resulting mixture was refluxed for 2 h. The solution was then cooled

down to r.t. and a solid precipitated out. This one was filtered, washed with ethanol (11.4 mL x 2) and dried to yield **27** (11.3 g, 58%) as a solid.

Step iii: To the solution of **27** (12 g, 29.9 mmol, 1 eq) in DCM/methanol (144 mL, 10:2) was added iodobenzene diacetate (13.48 g, 41.8 mmol, 1.4 eq) at r.t. under nitrogen atmosphere. The resulting mixture was stirred for 16 h. The solid was filtered off, washed with methanol (6 mL x 2) and dried to yield **28** (10.4 g, 87%) as solid.

Step iv: To the solution of **28** (0.2 g, 0.50 mmol) in dioxane/water (7 mL, 25:10) was added the corresponding boronic acid (0.60 mmol) and potassium carbonate (0.1 g, 0.75 mmol) at r.t. The mixture was degassed for 10 minutes. Bis (triphenylphosphine) palladium (II) dichloride (24 mg, 0.035 mmol) was then added at r.t. and the resulting mixture was heated to 110° C for 16 h. The solution was then cooled down to r.t. and concentrated under vacuum to remove dioxane. Water (5mL) was added to the reaction mixture and the solution was extracted with DCM (5mL x 2). Combined organic layers were washed with brine solution (3 mL), dried over anhydrous Na_2SO_4 and concentrated under vacuum. Crude compound was purified by column chromatography over silica gel 230-400 mesh by using 3% of methanol in DCM as an eluent to afford the desired compounds.

Spectrometric data of compounds **29** and **30** is given in table B.2 below.

B. Additional spectrometric data (^{1}H NMR and Mass):

1) Table B.1. Intermediates

Compound	Structure	NMR ^{1}H δ (ppm)
6a	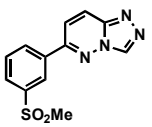	^{1}H NMR (400 MHz, $CDCl_3$), 9.14 (s, 1H); 8.52 (s, 1H); 8.26-8.21 (m, 2H); 8.07 (d, AH; J = 7.6); 7.73 (t, 1H; J = 8.0 Hz); 7.60 (d, 1H; J = 9.6 Hz); 3.07 (s, 3H).
7a	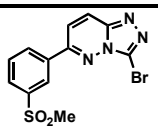	^{1}H NMR (400 MHz, $CDCl_3$), 9.12 (d, 1H; J = 9.6); 8.56 (s, 1H); 8.30 (d, 1H; J = 7.6 Hz); 8.14

		(d, 1H; J = 7.6 Hz); 7.90 (d, 1H; J = 9.6 Hz); 7.79 (t, 1H; J = 7.6 Hz); 3.10 (s, 3H).
6b	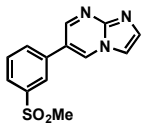	^{1}H (400 MHz, $CDCl_3$), 8.89 (d, 1H; J = 2.4 Hz); 8.80 (d, 1H; J = 2.4 Hz); 8.13 (s, 1H); 8.05 (d, 1H; J = 8.0Hz); 7.85 (d, 1H; J = 8.0 Hz); 7.80-7.74 (m, 2H); 7.65 (d, 1H; J = 2.0 Hz); 3.12 (s, 3H).
7b	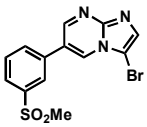	^{1}H (400 MHz, $CDCl_3$), 8.90 (d, 1H; J = 2.4 Hz); 8.82 (d, 1H; J = 2.4 Hz); 8.10 (s, 1H); 8.07 (d, 1H; J = 8.0 Hz); 7.90-7.85 (m, 2H); 7.77 (t, 1H; J = 8.0 Hz); 3.13 (s, 3H).
6c	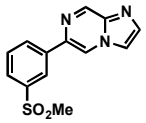	^{1}H NMR (400 MHz, $CDCl_3$), 9.20 (d, 1H; J = 1.2 Hz); 8.60 (d, 1H; J = 1.5 Hz); 6.51 (t, 1H; J = 1.8 Hz); 8.30 (dt, 1H; J = 7.7, 1.2 Hz); 7.98 (dt, 1H; J = 7.7, 1.2 Hz); 7.87 (d, 1H; J = 1.1 Hz); 7.80 (s, 1H); 7.71 (t, 1H; J = 7.7 Hz); 3.13 (s, 3H).
7c	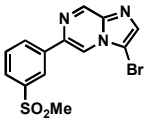	^{1}H NMR (400 MHz, $CDCl_3$), 9.14 (d, 1H; J = 1.5 Hz); 8.56 (t, 1H; J = 1.8 Hz); 8.48 (d, 1H; J = 1.5 Hz); 8.33 (d, 1H; J = 7.9 Hz); 8.01 (d, 1H; J = 7.9 Hz); 7.83 (s, 1H); 7.73 (t, 1H; J = 7.9 Hz); 3.13(s, 3H).
6d	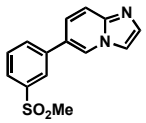	^{1}H NMR (400 MHz, $CDCl_3$), 8.43-8.40 (m, 1H); 8.15 (t, 1H; J = 2.0 Hz); 7.98-7.96 (m, 1H); 7.87-7.85 (m, 1H); 7.77 (d, 1H; J = 9.6 Hz); 7.73-7.67 (m, 3H); 7.46 (dd, 1H; J = 1.6, J = 9.6 Hz); 3.12 (s, 3H).
7d	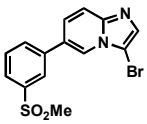	^{1}H NMR (400 MHz, $CDCl_3$), 8.34 (s, 1H); 8.19 (t, 1H; J = 2.0 Hz); 7.89 (dd, 1H; J = 1.6, J = 7.6 Hz); 7.77 (dd, 1H; J = 2.0, J = 7.6 Hz); 7.76-7.70 (m, 3H); 7.53 (dd, 1H; J = 1.6, J = 9.6 Hz);

		3.13 (s, 3H).
14a	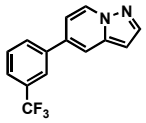	^{1}H NMR (400 MHz, $CDCl_3$), 8.50 (d, 1H; J = 8.4 Hz); 7.93 (d, 1H; J = 2.4 Hz); 7.80 (s, 1H); 7.71 (d, 1H; J = 8.0 Hz); 7.68 (s, 1H); 7.58 (d, 1H; J = 8.0 Hz); 7.52 (t, 1H; J = 8.0 Hz); 6.94 (dd, 1H; J = 2.0, J = 7.2 Hz), 6.53 (d, 1H; J = 2.0 Hz).
14d	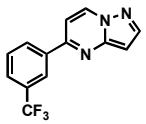	^{1}H NMR (400 MHz, $CDCl_3$), 8.76 (d, 1H; J = 7.2 Hz); 8.39 (s, 1H); 8.28 (d, 1H; J = 8.0 Hz); 8.17 (d, 1H; J = 2.0 Hz); 7.76 (d, 1H; J = 8.0 Hz); 7.65 (t, 1H; J = 8.0 Hz); 7.30 (d, 1H; J = 7.2 Hz); 6.77 (d, 1H; J = 2.0 Hz).
15d	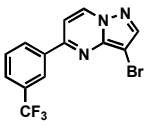	^{1}H NMR (400 MHz, $CDCl_3$), 8.71 (d, 1H; J = 7.2 Hz); 8.41-8.35 (m, 2H); 8.15 (s, 1H); 7.78 (d, 1H; J = 8.0 Hz); 7.67 (t, 1H; J = 8.0 Hz); 7.34 (d, 1H; J = 7.2 Hz).
20a	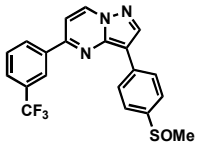	^{1}H NMR (400 MHz, $CDCl_3$), 8.80 (d, 1H; J = 7.2 Hz); 8.54 (s, 1H); 8.43-8.38 (m, 2H); 8.33 (d, 2H; J = 8.8 Hz); 7.82-7.75 (m, 3H); 7.71 (t, 1H; J = 8.0 Hz); 7.40 (d, 1H; J = 7.2 Hz); 3.08 (s, 3H).
14e	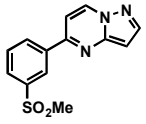	^{1}H NMR (400 MHz, $CDCl_3$), 8.85 (d, 1H; J = 7.2 Hz); 8.60 (s, 1H); 8.47-8.37 (m, 4H); 8.08 (d, 2H; J = 8.8 Hz); 7.85 (d, 1H; J = 8.0 Hz); 7.76 (t, 1H; J = 8.0 Hz); 7.47 (d, 1H; J = 7.2 Hz); 3.17 (s, 3H); ^{13}C (100 MHz, $CDCl_3$), 155.6, 144.0, 137.7, 137.5, 136.1, 1316, 130.6, 129.8, 128.0, 127.5, 126.5, 124.2, 109.3, 105.8, 44.7.

2) Table B.2. Final compounds:

Compound	Structure	NMR δ (ppm)	MS (EI)$^+$ m/z
8	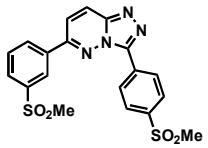	^{1}H (300 MHz, CD_3OD), 8.64 (s, 1H); 8.44 (d, 1H; J = 8.8 Hz); 8.38 (d, 1H; J = 8.8 Hz); 8.17 (d, 1H; J = 8.8 Hz); 8.03 (d, 1H; J = 8.8 Hz); 7.94 (m, 2H); 7.53 (d, 1H; J = 8.8 Hz); 3.07 (s, 6H).	429.1
9	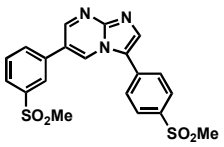	^{1}H (400 MHz, $CDCl_3$), 8.88 (d, 1H; J = 2.8); 8.79 (d, 1H; J = 2.4 Hz); 8.16 (d, 2H; J = 8.8 Hz); 8.13 (s, 1H); 8.08 (s, 1H); 8.08, 8.05 (d, 1H; J = 8.0 Hz); 7.86 (d, 1H; J = 8.0 Hz); 7.81 (d, 2H; J = 8.8 Hz); 7.77 (d, 1H; J = 8.0 Hz); 3.15 (s, 3H); 3.13 (s, 3H).	427.0
10	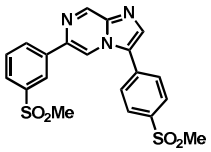	^{1}H (dmso-d_6, 400 MHz), 9.35 (d, 1H; J = 1.4 Hz); 9.19 (d, 1H; J = 1.4 Hz); 8.65 (t, 1H; J = 1.8 Hz); 8.46 (dd, 1H; J = 1.8, J = 7.8 Hz); 8.25 (s, 1H); 8.15 (d, 1H; J = 8.7 Hz); 8.13 (d, 1H; J = 8.7 Hz); 7.99 (dd, 1H; J = 1.8, J = 7.8 Hz); 3.32 (s, 3H); 3.29 (s, 3H).	427.0
11	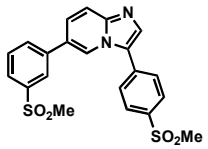	^{1}H (400 MHz, $CDCl_3$), 8.53 (s, 1H); 8.15 (d, 2H; J = 8.8 Hz); 8.10 (t, 1H; J = 2.0 Hz); 8.01 (d, 1H; J = 8.4 Hz); 7.97 (d, 1H; J = 9.6 Hz); 7.89 (s, 1H); 7.86-7.81 (m, 3H); 7.73 (t, 1H; J = 8.0 Hz); 7.62 (d, 1H; J = 9.6 Hz); 3.15 (s, 3H); 3.12 (s, 3H).	(ESI)$^+$ 427.0 $[M+H]^+$ 449.0 $[M+Na]^+$
17	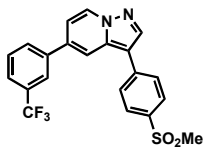	^{1}H NMR (400 MHz, $CDCl_3$), 8.62 (d, 1H; J = 7.2 Hz); 8.25 (s, 1H); 8.08-8.00 (m, 2H); 7.98 (d, 1H; J = 2.0 Hz); 7.88 (s, 1H); 7.86-7.79 (m, 3H); 8.08 (s, 1H); 7.70 (d, 1H; J = 7.6 Hz); 7.64 (t, 1H; J = 8.0 Hz); 7.13 (d, 1H; J = 7.2 Hz); 3.10 (s, 3H).	(ESI)$^+$ 417.0 $[M+H]^+$

20	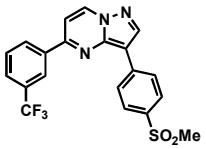	^{1}H (400 MHz, $CDCl_3$), 8.85 (d, 1H; J = 7.2 Hz); 8.60 (s, 1H); 8.47-8.42 (m, 1H); 8.40 (d, 1H; J = 8.4 Hz); 8.08 (d, 1H; J = 8.4 Hz); 7.85 (d, 1H; J = 7.2 Hz); 7.77 (t, 1H; J = 7.2 Hz); 7.46 (d, 1H; J = 7.2 Hz); 3.14 (s, 3H).	417.1
21	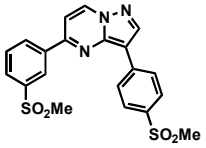	^{1}H (300 MHz, dmso-d_6), 9.38 (d, 1H; J = 7.5 Hz); 8.98 (s, 1H); 8.79 (t, 1H; J = 1.6 Hz); 8.71 (d, 1H; J = 7.9Hz); 8.53 (d, 2H; J = 8.6 Hz); 8.14 (d, 1H; J = 7.9 Hz); 8.01 (d, 2H; J = 8.6 Hz); 7.95 (d, 1H; J = 7.5 Hz); 7.91 (t, 1H; J = 7.9 Hz); 3.36 (s, 3H); 3.25 (s, 3H).	427.5
23	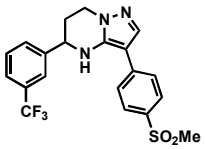	^{1}H (300 MHz, DMSO-d6), 7.86-7.61 (m, 9H) ; 6.96 (s, 1H) ; 4, 76-4, 66 (m, 1H) ; 4.20-4.08 (m, 1H), 3.96-3.83 (m, 1H) ; 3.17 (s, 1H) ; 2.34-2.13 (m, 2H).	$(ESI)^+$ 422.0 $[M+H]^+$ 444.0 $[M+Na]^+$
29	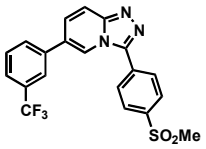	^{1}H (400 MHz, DMSO-d6), 8.89 (s, 1H), 8.32 (dd, 2H ; J = 1.8, J = 6.7 Hz), 8.15-8.17 (m, 2H), 8.11(d, , 1H ; J = 7.7 Hz), 8.03-8.06 (m, 1H), 7.91 (dd, , 1H, J = 9.5, J = 1.6 Hz), 7.74-7.83 (m, 2H), 3.33 (s, 3H). ^{13}C (100 MHz, DMSO-d_6), 116.3, 122.5, 123.2, 124.5, 124.5, 125.4, 125.4, 125.9, 126.8, 128.3, 129.4, 130.1, 130.5, 130.6, 130.8, 131.8, 132.1, 137.5, 142.1, 146.0, 150.3	$(ESI)^+$ 406.2 $[M+H]^+$
30	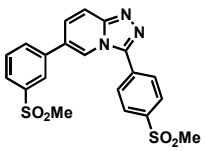	^{1}H (400 MHz, DMSO-d6), 8.90 (s, 1H), 8.29- 8.33 (m, 3H), 8.18 (s, 1H), 8.16 (s 2H), 8.08 (d, 1H, J = 9.6 Hz), 7.99 (d, 1H ; J = 8.2 Hz), 7.93 (dd, 1H, ; J = 1.5, J = 9.6 Hz), 7.78-7.82 (m, 1H), 3.32 (s, 6H). ^{13}C (100 MHz, DMSO-d_6), 115.9, 125.7, 126.2, 126.6, 127.8, 128.9, 129.0, 130.1, 131.3, 132.5, 137.2, 141.6, 145.6, 149.8	$(ESI)^+$ 428.2 $[M+H]^+$

* Unless otherwise specified

C. HPLC Methods

Using a XBridge C18 column, 1 µL injection volume, flow 1.2 mL/min; gradient: 25 – 100% B in 9 min (hold 5 min), 100 – 25% in 1 min (hold 6 min) (Mobile phase A: 10 mM buffer (Ammonium acetate/acetic acid) in H_2O and Mobile phase B: 10 mM buffer (Ammonium acetate/acetic acid) in CH_3OH with PDA – maximum chromatogram (210 – 400 nm).

D. Cytotoxicity data

Table D1.

Compd	IC_{50} (µM)		SI	
	CHO	vero	CHO	vero
1	>234	-	>30000	-
3	>240	-		-
12	27	-	700	-
18	>234	>234		
19	>221	-	100000	-
22	>226	-	53000	-
24	>219	-	3454	
31	17.9	195	1988	21666

E. In vitro ADME parameters

Compound in DMSO was spiked into either pH 6.5 phosphate buffer or 0.01M HCl (approx pH 2.0) with the final DMSO concentration being 1%. Samples were then analysed via Nephelometry to determine a solubility range as described by Bevan and Lloyd.[2]

1. Methods

1.1. Solubility

Compound in DMSO was spiked into either pH 6.5 phosphate buffer or 0.01M HCl (approx pH 2.0) with the final DMSO concentration being 1%. Samples were then analysed via Nephelometry to determine a solubility range as described by Bevan and Lloyd.[2]

1.2. Metabolic stability.

The metabolic stability assay was performed in duplicate in a 96-well micro titre plate. The test compounds (0.1 μM) were incubated (37 °C) in mouse, rat and pooled human liver microsomes (final protein concentration of 0.4 mg/mL; XenoTech, Lenexa, KS) suspended in 0.1 M phosphate buffer (pH 7.4) for predetermined time points, in the presence and absence of the cofactor NADPH (1mM). The reactions were quenched by the addition of ice cold acetonitrile containing internal standard (carbamazepine, 0.0236 μg/mL). The samples were centrifuged and the supernatant was analysed by means of LC-MS/MS (Agilent Rapid Resolution HPLC, AB SCIEX 4000 QTRAP MS). The relative loss of parent compound over time was monitored and plots were prepared for each compound of concentration versus time to determine the first order rate constant for compound depletion, which was used to calculate the degradation half-life, the *in vitro* intrinsic clearance value and subsequently a predicted *in vivo* intrinsic clearance value. The *in vivo* CL_{int} values were converted to a predicted *in vivo* hepatic extraction ratio (E_H). Metabolite searches were not conducted during the metabolic stability assay[3]. The same metod is used for both the turnover and the 5-point assay (E_H), the only difference being in the number of data points.

2. Results

Table E1.

Compound	Solubility (μM)		% remaining after 30 minutes (h/r/m)	E_H (h/r/m)
	pH2 (STD)	pH 6.5 (STD)		
1	<5	<5		<0.4/<0.3/<0.33
2	61 (2.4)	<5		
3	19 (6.0)	<5	84/100/92	-
4	<5	<5	95/88/100	<0.4/<0.3/<0.33

10	176 (0.9)	28 (2.9)	87/86/66	-
11	194 (0.5)	<5	100/100/87	-
12	191 (1.3)	<5	97/100/99	<0.4/<0.3/<0.33
17	<5	<5	100/95/100	-
18	<5	<5	100/100/100	<0.4/<0.3/<0.33
19	<5	<5	97/100/99	-
20	<5	<5	99/96/92	<0.4/<0.3/<0.33
21	<5	<5	99/98/68	-
22	<5	<5	100/87/72	<0.4/0.36/<0.33
24	122 (4.3)	<5	78/86/71	0.44/<0.3/0.39
31	<5	<5	8/7/24	-
Controls				
Reserpine	185 (1.4)	<5		
Hydrocortisone	194 (2.5)	186 (0.5)		

F. Metabolite identification

1. In vivo sample preparation

Frozen whole blood samples collected from rats dosed orally at 20 mg/kg and iv at 5 mg/kg were thawed and pooled separately. The pooled oral and iv blood samples were extracted by protein precipitation using 4 volumes of 0.1% FA in methanol; ultrasonicated and centrifuged. The resulting supernatant was concentrated at 40°C under nitrogen. The resulting extracts were filtered and injected on to the column (10 µl) for LC-MS analysis. Samples of blood collected from the rats before drug administration (pre-blood control) and analyte spiked in blood at 5000 ng/ml were also processed similarly.

2. In vitro incubations with rat liver microsomes (RLM)

The test compound (10 µM) was incubated at 37 °C in a solution containing 1 mg/ml microsomes (RLM male rat IGS, Xenotech), magnesium chloride (5 mM) and NADPH (1 mM) in phosphate buffer (100 mM, pH 7.4), for 1 hour while shaking. The samples were then prepared by protein precipation using 2 volumes of acetonitrile, centrifuged and filtered for LC-MS/MS analysis. Controls containing all the sample constituents (not incubated), and in which NADPH or microsomes were individually excluded were also prepared and handled similarly to the test sample.

LC-MS/MS analysis

LC-MS/MS analysis were performed on an 4000 QTRAP® (AB Sciex) equipped with a

Turbo V™ ion source and coupled to an Agilent 1200 Rapid Resolution HPLC system (600 bar, Agilent technologies, USA). 10 µL of samples stored on a sample tray set at 8°C were injected onto a Supelco Ascentis C18 column, (4.6 mm x 150 mm, 2.6 µm particles) at 40°C. Metabolites were separated using a gradient solvent system consisting of 0.1% formic acid (A) and 0.1% formic acid in acetonitrile (B). The gradient was as follows: 10% B for 0.5 min, 10-90% in 8.5 min, 90% B held for 3 min, and returned to initial conditions for 4 min to reequilibrate the column. The flow rate was 0.4 mL/min. The total run time per sample was 16 min.

All mass scans were operated under electrospray positive ionization mode and the operation parameters were as follows: curtain gas, 30 psi; collision gas, 6 psi; nebulizer gas (GS1), 50 psi; turbo gas (GS2), 60 psi; source temperature, 500°C; ion- spray voltage, 5000 V; declustering potential, 46V for 675615/31 and 121V for 674850/19; collisionally activated dissociation (CAD) gas setting: high. Enhanced mass spectrum was used as a survey scan to trigger information dependent acquisition of MS/MS spectra. The criteria for the information-dependent acquisition (IDA) were set for the most two intense peaks, which exhibited counts higher than 100000 cps. The scan speed for all scan functions was 4000 Da s^{-1}.

Metabolites formed in vivo were identified by comparison of oral and iv chromatograms with pre-blood control and metabolites formed in microsomal incubations were identified by comparison of chromatograms at 60 min with chromatograms at T0 and with no NADPH controls using Lightsight v2.3. The tentative identity of the metabolites was deduced by comparison of the product ion spectra of the $[M+H]^+$ ions of the metabolite with that of parent compound using Analyst 1.5.1. The retention time and fragmentation pattern was also compared to that of synthetic standards, where available, to confirm the identity.

Table F1: Metabolite identification summary for **31**

Drug and metabolites	**Retention time (min)**	**$[M+H]^+$ (*m/z*)**	**Diagnostic ions (m/z)**				**Tentative identity**
			A	**B**	**C**	**D**	

Parent **31**	8.0	437	374	347	269	242	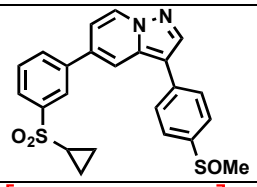
M1	6.8	469	390	363	285	258	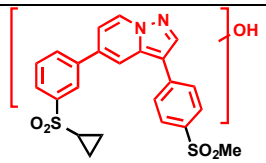
M2	7.1	469	390	347	285	242	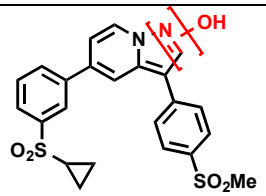
M3	7.4	469	390	363	285	258	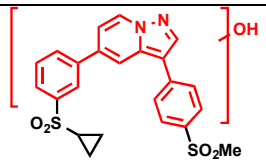
M4	8.0	469	390	363	285	258	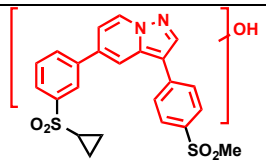
M5 (**19**)	8.5	453	374	347	269	242	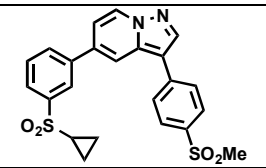

3. **Metabolite profiles of 31 in rats (A), of 31 in rat liver microsomes (B), of 19 in rats (C)**

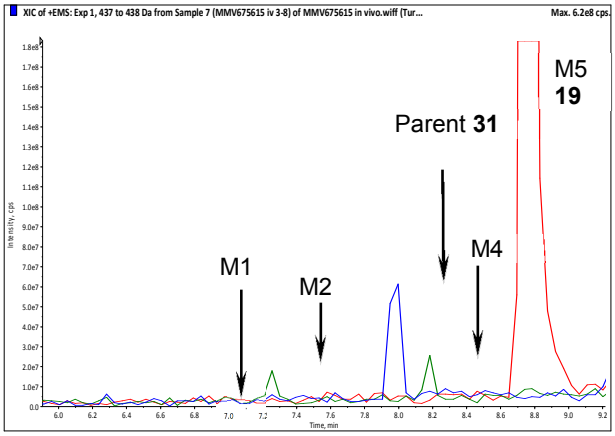

A

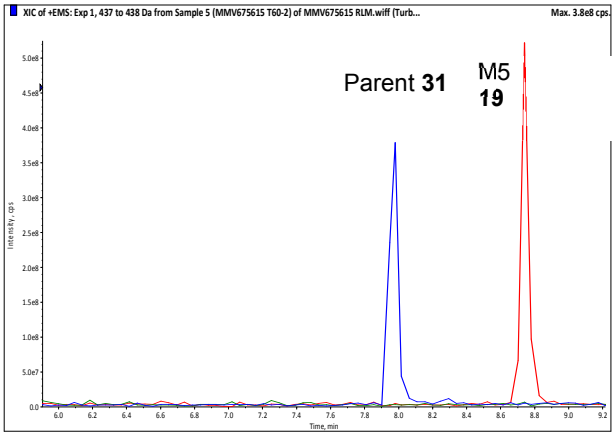

B

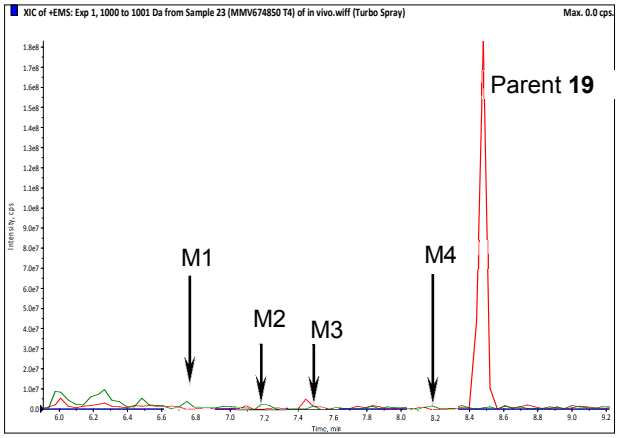

C

4. Proposed fragmentation patterns of 31 and 19

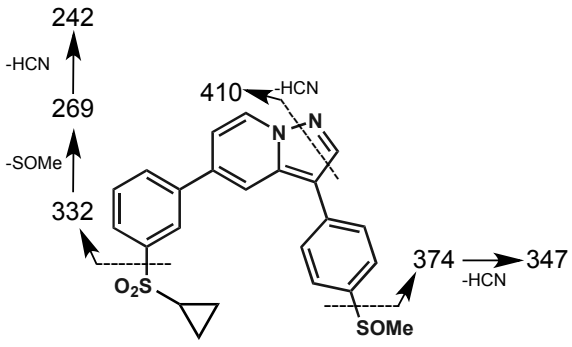

$[M+H]^+$ m/z= 437

31

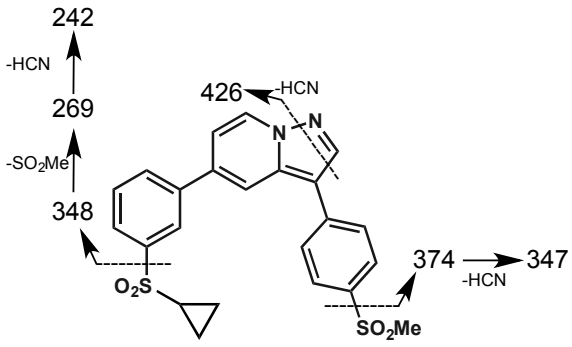

$[M+H]^+$ m/z= 453

19

G. SCID mouse model *in vivo* studies

The therapeutic efficacy of **31** against *P. falciparum* 3D7 was studied using a '4-day test' as previously described[4]. Briefly, NODscidIL2Rγ^{null} mice engrafted with human erythrocytes were infected with 20×10^6 *P. falciparum*-infected erythrocytes. Infections were performed by intravenous inoculation. All mice were randomly assigned to their corresponding treatment. The treatment started at day 3 and finished at day 6 after infection. In all cases, parasitemia was assessed in samples from peripheral blood obtained at days 3, 4, 5, 6, and 7 after infection.

The levels of **31** and **19** were evaluated in whole blood in order to determine standard pharmacokinetic parameters in the individuals of the efficacy study. Peripheral blood samples (25 μl) were taken at 0.25, 0.5, 1, 2, 4, 6, 8 and 23 hours after the first drug administration, mixed with 25 μL of H_2O mili Q and immediately frozen on dry ice. The frozen samples were stored at -80 ºC until analysis. Vehicle-treated mice experienced the same blood-sampling regimen. Blood samples were processed under standard liquid-liquid extraction conditions. Analysis by LC/MSMS is performed for quantification. The lower limit of quantification (LLOQ) in this assay was 0.001 $\mu g \cdot mL^{-1}$ for compounds **19** and **31**. Blood concentration *vs* time was analyzed by non-compartmental analysis (NCA) using Phoenix vers.6.3 (from Pharsight), from which exposure-related values (C_{max} and AUC_{0-t}) and t_{max} were estimated.

A qualitative analysis of the effect of treatment on *P. falciparum* Pf3D70087/N9 was assessed by microscopy and flow cytometry. Fresh samples of peripheral blood from *P. falciparum*-infected mice were stained with TER-119-Phycoerythrine (marker of murine erythrocytes) and SYTO-16 (nucleic acid dye) and then analyzed by flow cytometry (FACSCalibur, BD)[5]. Microscopy analysis was performed with Giemsa-stained blood smears from samples taken at days 5 and 7 (48 and 96 h after starting treatment, respectively).

Efficacy was expressed as the daily exposure (AUC, µg·h/ml per day) in whole blood or the daily dose administered (mg/kg) necessary to reduce parasitemia at day 7 by 90 % with respect to vehicle-treated mice (AUC_{ED90}). The AUC_{ED90} was estimated by fitting a four parameter logistic equation for the log_{10} [parasitemia at day 7 for each individual] *versus* the $AUC_{0\text{-}23h}$ of **31** and **19** in blood for each individual using GraphPad Prism 6.0.

All the experiments were approved by the DDW Ethical Committee on Animal Research and carried out in accordance with European Directive 2010/63/EU and the GSK Policy on the Care, Welfare and Treatment of Animals. The animal studies were performed at DDW Laboratory Animal Science facilities accredited by AAALAC. The human biological samples were sourced ethically and their research use was in accord with the terms of the informed consents.

H. *P.b.* liver assays

Parasites.

Plasmodium berghei Luciferase sporozoites were obtained by dissection of infected *A. stephensi* mosquito salivary glands supplied by the New York University Insectary. Dissected salivary glands were homogenized in a glass tissue grinder and filtered twice through nylon cell strainers (40 µm pore size, BD Falcon) and counted using a hemocytometer. The sporozoites were kept on ice until needed.

Cell lines.

HepG2-A16-CD81EGFP cells stably transformed to express a GFP-CD81 fusion protein[7], were cultured at 37°C in 5% CO2 in DMEM (Invitrogen, Carlsbad, USA) supplemented with 10% FCS, 029 mg/mL glutamine, 100 units penicillin and 100 µg/mL streptomycin.

Sporozoite invasion assay.

P. berghei is able to infect human hepatocarcinoma HepG2 cells expressing the tetraspanin CD81 receptor[6,7]. 3x103 HepG2-A16-CD81EGFP cells in 5 µL of medium (2x105 cells/ml, 5%FBS, 5xPen/Strep/Glu) were seeded in 1536-well plates (Greiner BioOne white solid bottom) 20-26 hours prior to the actual infection. 18 hours prior to

infection, 50 nL of compound in DMSO (0.5% final DMSO concentration per well) were transferred with a PinTool (GNF Systems) into the assay plates (10 µM final concentration). Atovaquone (10 µM) and 0.5% DMSO were used as positive and negative controls, respectively. *P. berghei* Luciferase sporozoites were freshly dissected from infected *A. stephensi* mosquito salivary glands and filtered twice through a 40 µm nylon pore cell strainer. The sporozoites were re-suspended in media, counted in a hemocytometer and their final concentration adjusted to 200 sporozoites per µL. Also, penicillin and streptomycin are added at 5x-fold increased concentration for a final 5x-fold increased concentration in the well. The HepG2-A16-CD81EGFP cells were then infected with $1x10^3$ sporozoites per well (5 µL) with a single tip Bottle Valve liquid handler (GNF), and the plates spun down at 37°C for 3 minutes in an Eppendorf 5810 R centrifuge with a centrifugal force of 330x on lowest acceleration and brake setting. After incubation at 37°C for 48 hours the EEF growth was quantified by a bioluminescence measurement. The increased antibiotic concentration did not interfere with the parasite or HepG2-A16-CD81EGFP growth. Atovaquone and naive wells were used as controls on each plate. The compounds were screened in a 12 point serial dilution to determine their exact IC_{50} values.

Bioluminescence quantification of exo-erythrocytic forms (EEFs).

Media was removed by spinning the inverted plates at 150xg for 30 seconds. 2 µL BrightGlo (Promega) were dispensed with the MicroFlo (BioTek) liquid handler. Immediately after addition of the luminescence reagent, the plates were read with the Envision Multilabel Plate Reader (PerkinElmer). IC_{50} values were obtained using measured bioluminescence intensity and a non-linear variable slope four parameter regression curve fitting model in Prism 6 (GraphPad Software Inc).

I. Additional references

(1) Davies, B. and Morris, T. Physiological parameters in laboratory animals and humans, *Pharm. Res*. 1993, *10*, 1093-1095.

(2) Bevan, C. D. and Lloyd, R. S. A High-Throughput Screening Method for the Determination of Aqueous Drug Solubility Using Laser Nephelometry in Microtiter Plates, *Anal. Chem.* **2000**, *72,* 1781-1787.

(3) Obach, R.S. Prediction of human clearance of twenty-nine drugs from hepatic microsomal intrinsic clearance data: An examination of in vitro half-life approach and non-specific binding to microsomes. *Drug Metab. Dispos.* **1999**, *27*, 1350-1359.

(4) Jiménez-Díaz, M. B.; Mulet, T.; Viera, S.; Gómez, V.; Garuti, H.; Ibáñez, J.; Alvarez-Doval, A.; Shultz, L. D.; Martínez, A.; Gargallo-Viola, D.; Angulo-Barturen, I. Improved Murine Model of Malaria Suing Plasmodium Falciparum Competent Strains Null Mice Engrafted with Human and Non-Myelodepleted NOD- Scid IL2Rγnull Mice Engrafted with Human Erythrocytes. *Antimicrob. Agents Chemother.* **2009**, *53*, 4533–4536.

(5) Jiménez-Díaz, M. B.; Mulet, T.; Gómez, V.; Viera, S.; Alvarez, A.; Garuti, H.; Vázquez, Y.; Fernández, A.; Ibáñez, J.; Jiménez, M.; Gargallo-Viola, D.; Angulo-Barturen, I. Quantitative Measurement of Plasmodium-Infected Erythrocytes in Murine Models of Malaria by Flow Cytometry Using Bidimensional Assessment of SYTO-16 Fluorescence. *Cytom. Part A* **2009**, *75*, 225–235

(6) S. Yalaoui *et al*., Hepatocyte permissiveness to *Plasmodium* infection is conveyed by a short and structurally conserved region of the CD81 large extracellular domain. *PLoS Pathog.* **4**, e1000010 (2008).

(7) O. Silvie *et al*., Hepatocyte CD81 is required for *Plasmodium falciparum* and *Plasmodium yoelii* sporozoite infectivity. *Nat. Med.* **9**, 93 (2003).